

Not all vaping is the same: Differential pulmonary effects of vaping cannabidiol versus nicotine

Online Supplement

Supplemental Methods:

Flow cytometry

The right lung lobe from each animal was digested in collagenase IV/DNase I solution to isolate leukocytes (references E5-E8). Immune cells were stained with cell type-specific antibodies for flow cytometry analysis to determine the numbers and phenotype of various immune subsets (references E5-E8). For intracellular staining, cells were treated with permeabilizing solution (BD Biosciences) and then stained with specific antibodies as described previously (references E6, E7). Samples were acquired using LSRII-A flow cytometer and data analyzed by FlowJo software. List and source of fluorochrome conjugated antibodies is provided in **Table E4** and the gating strategy is shown in **Figure 5E** in online supplement.

Lung histology

Left lung lobes from all mice were sent to IDEXX BioAnalytics in 10% formalin and processed as reported previously (reference E5). Each lung lobe was trimmed to provide a piece of lung for cryomicrotomy. The remaining lung tissue was processed for paraffin embedding, sectioned and stained with hematoxylin and eosin (H&E). All sections were examined microscopically by a veterinary pathologist. Microscopic changes that were observed in the lung were graded, as to severity, using a modification of a published scoring system for evaluation of lung changes in mouse lung models of acute pneumonia (reference E9). Morphologic changes were chosen based on reports of vaping-related pathologies (reference E10).

Multiplex cytokine/chemokine assay

Concentrations of various cytokines/chemokines in the BAL were measured by Luminex multiplex cytokine/chemokine assay using MILLIPLEX MAP Kit (Millipore, Cat# MCYTOMAG-70K-27) following the manufacturer's instructions. Data acquisition was performed on FLEXMAP 3D (Luminex Corp. Austin, TX, USA). During data analysis, limit of detection (LOD) was used for any data points with values <LOD.

Total BAL protein determination

The level of total proteins in the BAL was determined by BCA protein assay kit (Cat#23225) from Pierce as per manufacturer's protocol.

Albumin leak measurement

The levels of albumin in the BAL were quantified by ELISA using Bethyl Laboratories (Montgomery, TX, USA) reagents and plates were developed with 3,3',5,5'-tetramethylbenzidine (TMB) from eBioscience Inc. (San Diego, CA, USA), and absorbance read at 450 nm as described previously (references E5-E8).

***In vivo* FITC-dextran leak measurement**

Systemic leak of FITC-dextran from lungs of animals, as an index of lung endothelial damage, was determined by intratracheally instilling mice with a 50 μ L aliquot of 200 mg/mL FITC-dextran in 1x PBS (10 μ g/mouse). One hour later, mice were bled to collect the plasma by centrifugation, and FITC fluorescence in plasma was measured using Exci485/Emi528 wavelengths in a Synergy H1 Hybrid plate Reader (BioTek). Fluorescence values were calculated using slope and intercept measurements from a standard curve.

Neutrophil elastase (NE) assay

Neutrophil elastase (NE) levels in the BAL and lungs were quantified by using Neutrophil Elastase/ELA2 DuoSet ELISA kit (DY4517-05) from R&D Systems (Minneapolis, MN, USA) following the manufacturers protocol.

Myeloperoxidase (MPO) assay

In this assay, MPO generates HClO (hypochlorous acid) from H₂O₂ and Cl⁻, that reacts with taurine to generate taurine chloramine. Taurine chloramine subsequently reacts with chromophore TNB to eliminate the color at 412 nm and the absorbance is inversely proportional to the amount of MPO enzyme present in the sample. Briefly, enzyme reaction for each sample was initiated in the presence or absence of MPO substrate in a 96-well ELISA plate and incubated at 25°C for 1 hour according to the manufacturer's protocol. This incubation generated taurine chloramine. The reaction was stopped by adding a stop mix reagent and plate incubated at room temperature for another 10 minutes. TNB reagent was then added to all samples and incubated for 10 minutes at room temperature.

Absorbance at 412 nm was recorded in Synergy H1 Hybrid plate Reader (BioTek)". Data are depicted as the difference in the absorbances at OD_{412nm} in each sample after the reaction was carried either in the presence or absence of the substrate and calculated as $A_{412nm} = (A_{412nm})_{\text{sample blank}} - (A_{412nm})_{\text{sample}}$.

Oil Red O Staining of BAL cells and lung tissue

Oil Red O strongly stains lipids in cells and is readily visualized by bright field and fluorescent microscopy. Cells were stained with oil Red O stain as described previously (reference E5). Briefly, cells in BAL were harvested, washed and live/dead cell counts performed using trypan blue dye. Cytospin slides were prepared by cytocentrifuging 50×10⁴ live BAL cells in 100 µL of 10% fetal calf serum in PBS at 1500 rpm for 5 min. Slides were air-dried for 10 min at room temperature and then

fixed in 3.7% paraformaldehyde in Hanks' balanced salt solution for 10 min at room temperature. Slides were gently washed twice in distilled water and then placed in absolute propylene glycol for 5 min. This was followed by staining with 0.5% oil Red O solution (Cat# O1516, Sigma Aldrich, St. Louis, MO) for 10 min at 60°C temperature. Slides were rinsed for 5 min in 85% propylene glycol, washed twice in distilled water and counterstained with hematoxylin solution for 30 secs to stain nuclei. Slides were mounted with aqueous mounting medium and red-stained cells counted by scoring at least 10 microscopic fields at 200x magnification. For tissue histology, mouse lung tissues (left lung lobes) were sent to IDEXX BioAnalytics (IDEXX BioAnalytics, Atlanta, GA, USA) in 10% formalin and processed for staining as described previously (references E5). Briefly, lung tissue was trimmed to provide a piece for cryomicrotomy. Lung tissue for cryomicrotomy was snap-frozen in optimal cutting temperature (OCT), sectioned on a cryostat and stained with Oil Red O. All sections were examined microscopically by a veterinary pathologist.

Antioxidant Assay

Antioxidant capacity in the BAL and lung lysates was measured using Cayman's antioxidant assay kit (Cat# 709001, Ann Arbor, MI, USA) that relies on the ability of antioxidants in the sample to inhibit the oxidation of ABTS® (2,2'-Azino-di-[3-ethylbenzthiazoline sulphonate]) to ABTS^{®+•} by metmyoglobin. The amount of ABTS^{®+•} produced was monitored by reading the absorbance at 750 nm in Synergy H1 Hybrid plate Reader (BioTek). The antioxidants in the sample cause suppression of the absorbance at 750 nm to a degree which is proportional to their concentration. The capacity of the antioxidants in the sample to prevent ABTS® oxidation is compared with that of Trolox standard, a water-soluble tocopherol analogue, and is quantified as millimolar Trolox equivalents.

Isolation of human neutrophils.

Human neutrophils were purified from the peripheral whole blood from donors using a Miltenyi Biotec MACSxpress Whole Blood Neutrophil Isolation Kit following a step-by-step protocol from the manufacturer (Cat. No. 130-104-434, Miltenyi Biotec). Multiple human donors kindly provided the whole blood, four Asian Americans (one female and three males) and four Caucasian Americans (one female and three males). Subject ages varied from 28 years to 59 years.

***In-Vitro* Exposure Conditions**

Cells in *in vitro* assays were directly exposed to freshly generated aerosol puffs in a closed exposure system where air-liquid interface (ALI) chambers were kept inside a 37°C incubator. For ALI experiments, we used the same closed-system vaping devices and refill liquid formulations as used during *in vivo* exposure experiments. Aerosols from CBD-containing Calm-Vape and nicotine-containing Juul (Nic-Vape) were generated using a Borgwaldt LX-1 (Richmond, VA, United States) single-port piston-operated machine. All ALI exposures were done for 1 hour, after which cells were provided with fresh complete culture media and transferred to 37°C degrees, CO₂ incubator for 24-hour recovery, following which assays were performed (see below). During cell exposure to machine-generated aerosols, the basal side of the permeable support was constantly submerged in serum-free media so that basal side of the cells remains in contact with the media for the entire duration of the exposure. Cells used in *in vitro* experiments were directly exposed to freshly generated puffs. Before performing the actual experiments, we standardized the puff-protocol using these cell types for a particular cell-density. Our standardized exposure conditions closely match the Health Canada Intense (HCI) puffing protocol and was a 3-sec puff every 30 sec, with a 55-ml puff volume. We estimated that each puff delivered approximately 55.9 µg CBD and 62.2 µg nicotine. Cells were exposed to 110 total puffs over the period of 1 hour. Each puff was automatically initiated by vaping devices. ALI chamber was cleaned with methanol and distilled water between each of the four

exposure conditions. A detailed schema of our *in vitro* exposure system has been published previously (E2) (https://tobaccocontrol.bmj.com/content/25/Suppl_2/ii81.long#DC2).

***In Vitro* exposures and Cytotoxicity Assays**

Human small airway epithelial cells (SAEC) (LONZA, USA; Catalog #: CC-2547S) were cultured in complete growth medium (LONZA, USA bullet kit (Catalog #: CC-3118)) to confluence. Cells were harvested and seeded onto 6-well culture inserts (0.5 million cells/well (for FITC-dextran permeability assay, 1 million cells/insert)) overnight before exposures. For purified human neutrophil assays, fresh patient-derived neutrophils were harvested and immediately seeded onto 6-well culture inserts (0.8 million cells/well) in RPMI-1640 culture media, neutrophils don't attach but remain in suspension and need to be seeded onto culture inserts at a density/volume that is sufficient, to make a monolayer on the surface of the insert for the ALI exposures. Cells were directly exposed for 1 hour to air, nicotine-containing aerosols or CBD aerosols using a closed air-liquid interface (ALI) system in which apical surface of cells does not touch medium while basolateral side remains in contact with the serum-free media in the bottom chamber. Aerosols from CBD Calm-Vape and nicotine-containing Juul pods were generated using a Borgwaldt LX-1 (Richmond, VA, United States) single-port piston-operated smoking machine. The Juul device was used to aerosolize both the products. Exposure protocol followed was as follows: 3-sec puff duration every 30 seconds in a 55 mL puff volume for a total of 110 puffs over the period of 1 hour. CBD and nicotine products used for *in vitro* experiments were identical to those used for *in vivo* experiments. We have estimated that each puff in ALI exposures contained approximately 55.9 µg CBD and 62.2 µg nicotine. At the end of 1-hour exposures in ALI system, inserts with human SAECs and neutrophils were removed from ALI chambers, transferred to new 6-well plates with fresh complete media, and incubated in a 37°C incubator with 5% CO₂ for 24 hours. SAEC cytotoxicity was determined by trypan blue-dye exclusion and lysosomal neutral red dye uptake procedures. Trypan blue dye stains dead cells that can be counted under bright-field

microscope, while neutral red dye stains lysosomes in viable cells which can be scored by measuring the absorbance of cell-extracted dye at 540 nm following the manufacturer's instructions (Bio Vision, USA). Neutrophil cytotoxicity was measured by trypan blue dye-exclusion assay as well as by Annexin V-FITC detection apoptosis assay using a kit from Invitrogen (Invitrogen, USA) following manufacturer's instructions. Unexposed neutrophils as experimental control was kept in growth media in the incubator for the entire duration of the experiment.

For human neutrophil experiments, cells from multiple donors were utilized as follows: For trypan blue method: **a)** Unexposed control n=6 independent experiments performed in triplicate representing technical replicates (n=6 donors); **b)** Air control and Nic-Vape exposures, n=7 independent experiments performed in triplicate (n=7 donors); **b)** CBD-Vape n= 8 independent experiments done in triplicate (n=8 donors). For apoptosis assay: n=5 independent experiments done in triplicate per exposure group (n=5 donors). For NE assay: n=6 independent experiments done in triplicate per group (n=6 donors). Experiments with human SAECs were done three independent times in triplicate using 3 different commercial cell vials (ampoules) from LONZA, and these cells were from two donors, one vial from a healthy 56-year-old Hispanic male and two vials from a healthy 40-year-old Caucasian male.

FITC-dextran permeability assay

One million human SAECs/culture insert in a 6-well plate format were cultured in complete growth media overnight and next day directly exposed at the air-liquid interface (ALI) to 110 puffs of air, nicotine or CBD aerosols for 1 hour (3-sec puff duration) as described above for "*in vitro* cytotoxicity assays". Upon completion of the exposures, FITC-dextran at 10 mg/mL concentration in phenol-free high glucose Dulbecco's Minimum Essential Medium with L-glutamine and HEPES was added to the apical chamber, FITC-free media was added in the bottom chamber and incubated for 2.5 hours. Samples were harvested from the basolateral chamber (bottom chamber) and fluorescence was

quantified using Exci485/Emi528 wavelengths in a Synergy H1 Hybrid plate Reader (BioTek). The paracellular permeability was quantified by measuring the FITC-dextran concentration in samples from basolateral chamber by employing a standard curve.

Supplemental References:

- E1.** Goniewicz ML, Kuma T, Gawron M, Knysak J, Kosmider L. Nicotine levels in electronic cigarettes. *Nicotine Tob Res* 2013;15(1):158-66.
- E2.** Leigh NJ, Lawton RI, Hershberger PA, Goniewicz ML. Flavourings significantly affect inhalation toxicity of aerosol generated from electronic nicotine delivery systems (ENDS). *Tob Control* 2016;25(2):ii81-ii87.
- E3.** Goniewicz ML, Boykan R, Messina CR, Eliscu A, Tolentino J. High exposure to nicotine among adolescents who use Juul and other vape pod systems ('pods'). *Tob Control* 2019;28(6):676-677.
- E4.** Kosmider L, Sobczak A, Fik M, Knysak J, Zaciera M, Kurek J, Goniewicz ML. Carbonyl compounds in electronic cigarette vapors: effects of nicotine solvent and battery output voltage. *Nicotine Tob Res*. 2014 Oct;16(10):1319-26. doi: 10.1093/ntr/ntu078. Epub 2014 May 15. PMID: 24832759; PMCID: PMC4838028.
- E5.** Bhat TA, Kalathil SG, Bogner PN, Blount BC, Goniewicz ML, Thanavala YM. An Animal Model of Inhaled Vitamin E Acetate and EVALI-like Lung Injury. *N Engl J Med* 2020;382(12):1175-1177.
- E6.** Bhat TA, Kalathil SG, Leigh L, Muthumalage T, Rahman I, Goniewicz ML, Thanavala YM. Acute Effects of Heated Tobacco Product (IQOS) Aerosol Inhalation on Lung Tissue Damage and Inflammatory Changes in the Lungs. *Nico & Tob Res* 2021;23(7):1160-1167.

- E7.** Bhat TA, Kalathil SG, Bogner PN, Miller A, Lehmann PV, Thatcher TH, Phipps RP, Sime PJ, Thanavala Y. Secondhand Smoke Induces Inflammation and Impairs Immunity to Respiratory Infections. *J Immunol* 2018;200(8):2927-2940.
- E8.** Bhat TA, Kalathil SG, Bogner PN, Lehmann PV, Thatcher TH, Sime PJ, Thanavala Y. AT-RvD1 Mitigates Secondhand Smoke-Exacerbated Pulmonary Inflammation and Restores Secondhand Smoke-Suppressed Antibacterial Immunity. *J Immunol* 2021;206(6):1348-1360.
- E9.** Dietert K, Gutbier B, Wienhold SM, Reppe K, Jiang X, Yao L, et al. Spectrum of pathogen- and model-specific histopathologies in mouse models of acute pneumonia. *PLoS One* 2017;12(11):e0188251.
- E10.** Butt YM, Smith ML, Tazelaar HD, Vaszar LT, Swanson KL, Cecchini MJ, et al. Pathology of Vaping-Associated Lung Injury. *N Engl J Med* 2019;381(18):1780-1781.

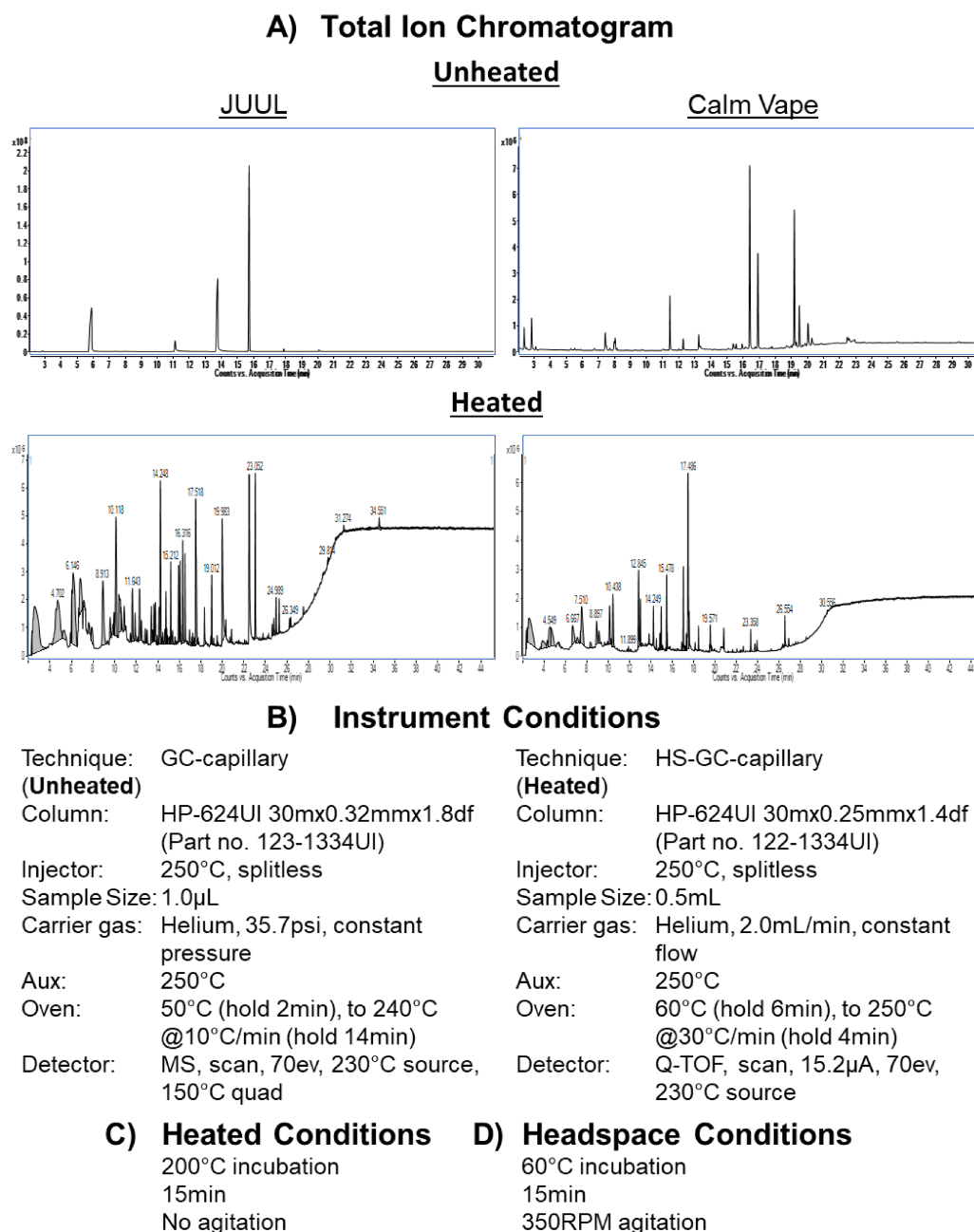


Figure E1. Results of chromatography analysis of vaping products used in the study. CBD, nicotine, and flavoring chemicals were identified and measured in each vaping product using gas chromatography/mass spectrometry (GC/MS) methods, as described previously (supplemental references E1, E2). GC/MS analysis showed that the primary cannabinoid in CalmVape product was CBD as listed on the packaging (43.9 mg/mL) and this product did not contain delta-9 tetrahydrocannabinol (THC). Nicotine concentration in Juul vaping product was 48.9 mg/mL (reference E3).

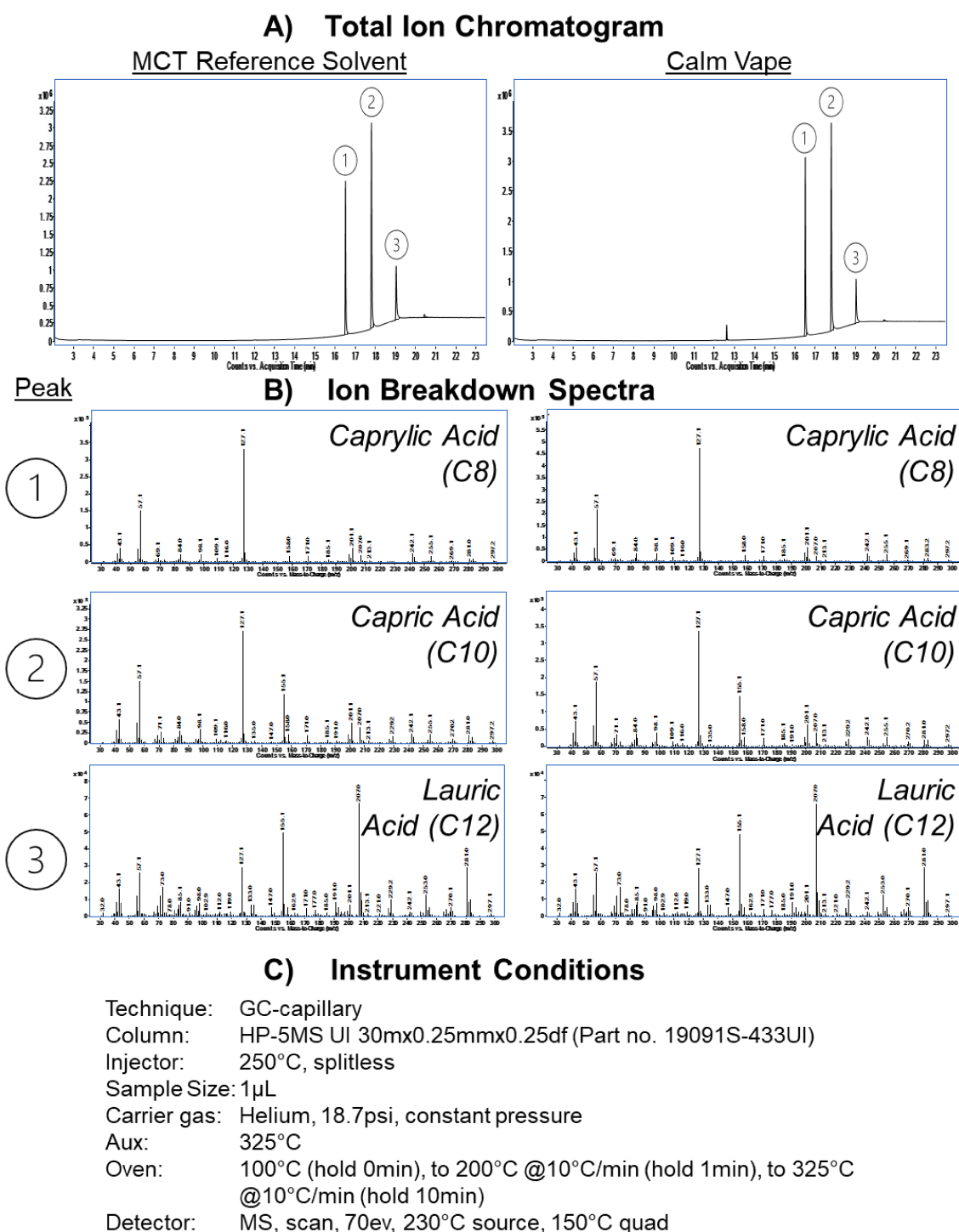
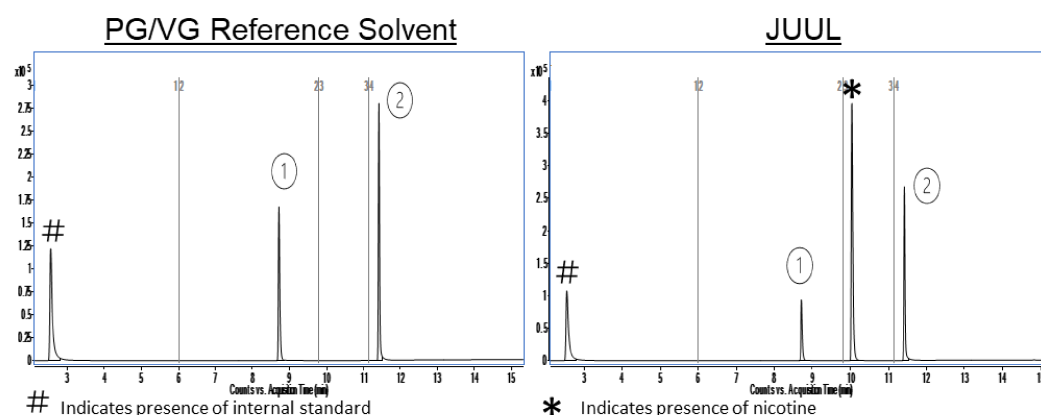


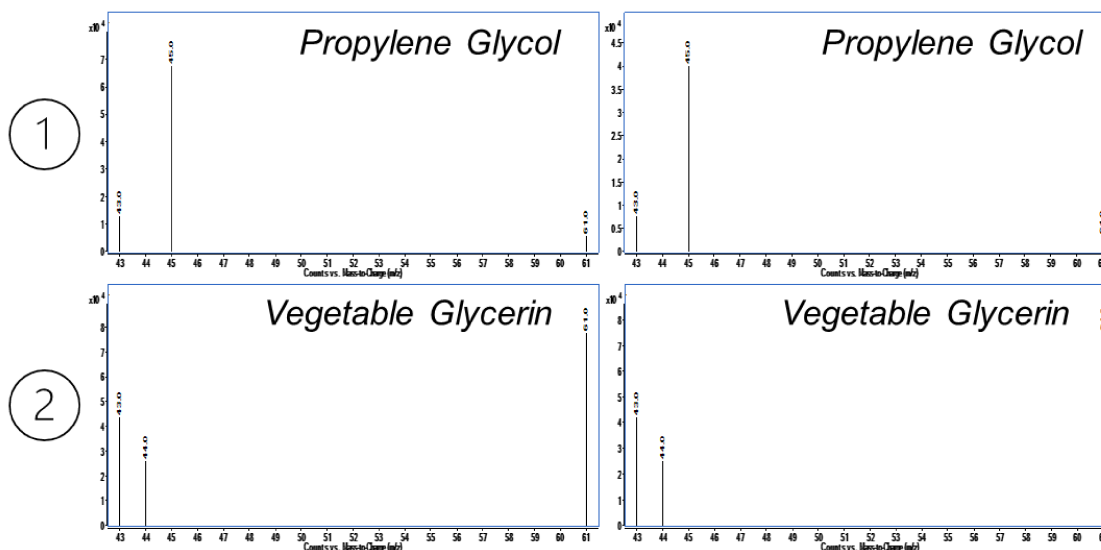
Figure E2. Identification of solvents used in CalmVape product (CBD-Vape). We confirmed the presence of medium chain triglycerides (MCT) in CalmVape product. No PG or VG have been found.

A) Total Ion Chromatogram



Peak

B) Ion Breakdown Spectra



C) Instrument Conditions

Technique: GC-capillary
 Column: HP-WAX UI 30m x 0.25mm x 0.25 df (Part no. 122-7032UI)
 Injector: 250°C, 75:1 split
 Sample Size: 1µL
 Carrier gas: Helium, 1.2mL/min, constant flow
 Aux: 250°C
 Oven: 60°C (hold 6min), to 250°C @30°C/min (hold 4min)
 Detector: MS, SIM, PG @ 10.00min (43,45,61 amu) VG @ 12.50min (43,44,61 amu), 70ev, 230°C source, 150°C quad

Figure E3. Identification of solvents used in Juul product (Nic-Vape). We confirmed presence of PG and VG. No medium chain triglycerides (MCT) have been found.

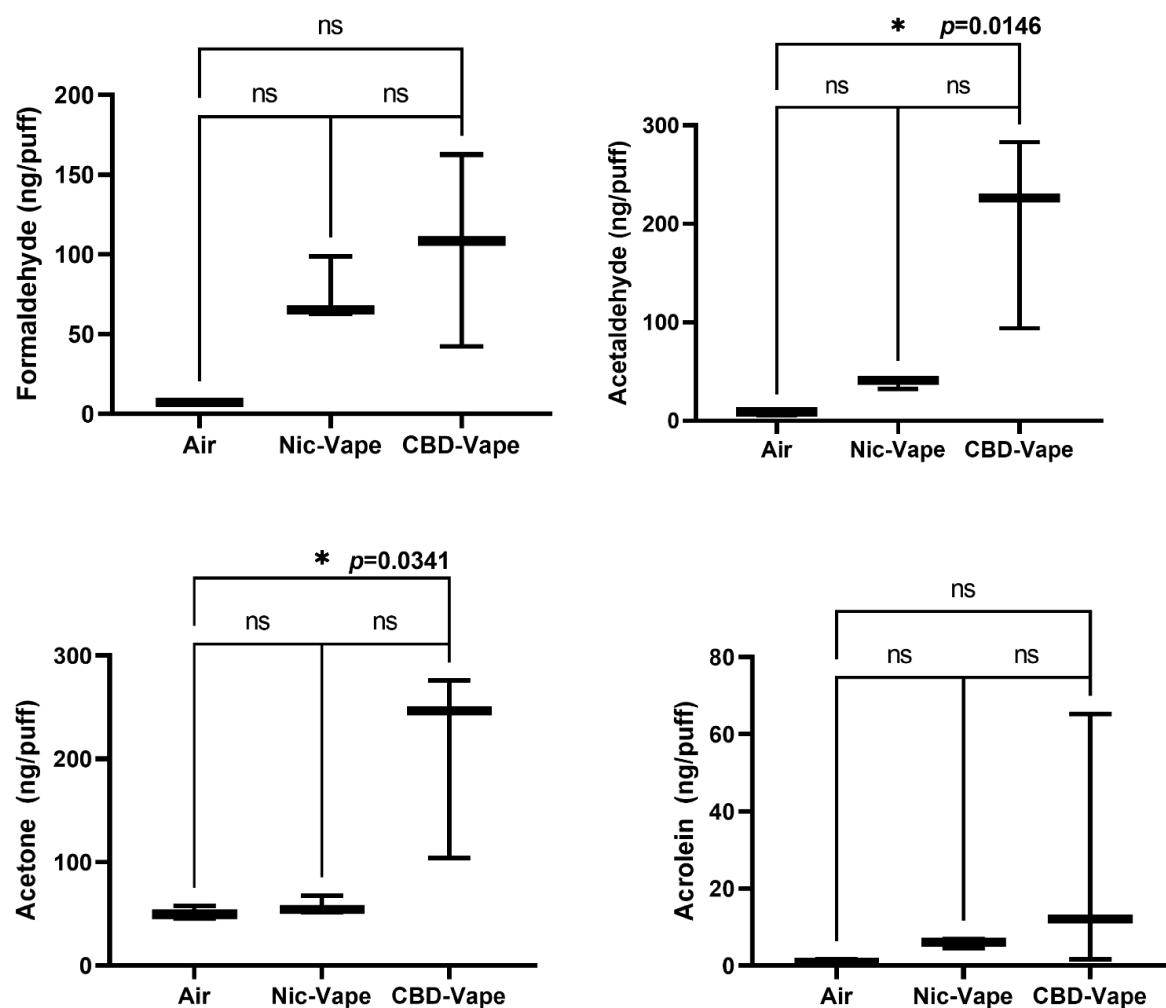


Figure E4. Levels of potentially toxic carbonyl compounds (formaldehyde, acetaldehyde, acetone, and acrolein) in aerosol generated from both vaping products [reference E4] and air (control). Increased levels of carbonyl compounds emitted from vaping products have been associated with thermal degradation of solvents used in liquids.

Table E1. Flavoring chemicals identified in both vaping products. Juul product also contained benzoic acid used to create nicotine salt (nicotine benzoate).

JUUL			Calm Vape		
<u>Analyte name</u>	<u>CAS</u>	<u>Flavor Descriptor</u> ¹	<u>Analyte name</u>	<u>CAS</u>	<u>Flavor Descriptor</u> ¹
Amylene hydrate	75-85-4	pungent	Amylene hydrate	75-85-4	pungent
2-Propanol, 1,1'-oxybis-	110-98-5	very mild, alcoholic	Benzyl Alcohol	100-51-6	chemical, fruity cherry, almond, balsamic, bitter
Benzaldehyde, 3,4-dimethoxy-	120-14-9	sweet, creamy, vanilla-like	Carvone	6485-40-1	sweet, minty, spearmint, carvone, caraway
Azolidine	123-75-1	ammonia and fishy, amine-like with seaweed and shellfish nuances	Linalool	78-70-6	citrus, orange, lemon, floral, waxy, aldehydic, woody
Benzoic Acid	65-85-0	faint balsam	Caryophyllene	87-44-5	spicy, clove, woody, nut skin powdery, peppery
Triethyl citrate	77-93-0	odorless to mild fruity wine	Octanoic acid	124-07-2	rancid, soapy, cheesy, fatty, brandy
Butyrolactone	96-48-0	milky, creamy with fruity peach-like afternotes	Decanoic acid, methyl ester	110-42-9	fatty, oily, fruity
			Octanoic acid, methyl ester	111-11-5	green, fruity, waxy, citrus, aldehydic and fatty
			Caryophyllene oxide	1139-30-6	dry, woody, cedar, old wood, carrot, ambrette
			Cherry propanol	1197-01-9	fruity, cherry, sweet, hay-like with cereal and bread-like nuances
			Cis-carveol	1197-06-4	caraway
			Ethanone, 1-(4-methylphenyl)-	122-00-9	sweet, creamy, fruity, cherry and heliotropine-like

¹Flavor descriptors determined from The Good Scents Company (<http://www.thegoodscentscompany.com/index.html>)

Table E2. Chemical names of potential thermal degradation by products identified in heated solutions (200°C for 10 mins).

JUUL		Calm Vape	
Analyte name	CAS	Analyte name	CAS
Ethanol, 2,2'-oxybis-, dipropionate	6942-59-2	Propionaldehyde	123-38-6
1,3-Dioxane	505-22-6	1,5,5-Trimethyl-6-methylene-cyclohexene	514-95-4
Pyridine	110-86-1	2H-Pyran, 3,4-dihydro-	110-87-2
Propionaldehyde	123-38-6	Cyclohexanol, 1-methyl-	590-67-0
Thiocyanic acid, ethyl ester	542-90-5	Menthatriene <1,3,8-para->	18368-95-1
Cyclopenta[c]pentalen-3(3aH)-one, 1,2,5a,6,7,8-hexahydro-6,6-dimethyl-	91531-59-8	Cyclohexa-1,4-diene <1-methyl->	4313-57-9
Pyridine <2-acetyl->	1122-62-9	Cymenene <para->	1195-32-0
Benzoic acid, methyl ester	93-58-3	p-Mentha-1,5,8-triene	21195-59-5
4-(2,4,4-Trimethyl-cyclohexa-1,5-dienyl)-but-3-en-2-one	1000187-51-9	Cyanamide, dimethyl-	1467-79-4
2,4,6-Cycloheptatrien-1-one, 2-methoxy-	2161-40-2	Crotonaldehyde <3-methyl->	107-86-8
Phenol, 2-amino-5-methyl-	2835-98-5	Cycloheptatriene	544-25-2
Phenyl alcohol	108-95-2	1-Methylcyclohexa-1,3-diene	1000298-96-0
3-Pyridinamine, 2,6-dimethyl-	3430-33-9	Benzene, 1,4-diethyl-	105-05-5
Hexane, 3,3,4,4-tetrafluoro-	648-36-2	Cycloheptanol	502-41-0
Pyrazine <2-acetyl->	22047-25-2	Cyclohexanol, 2-methyl- (isomer I)	583-59-5
Methanesulfonic anhydride	7143-01-3	.+/-.-trans-2-Cyclohexene-1,4-diol	41513-32-0
DL-Norleucine amide, N,N,N'-tetramethyl-	1000453-48-5	Butyl 4,7,10,13,16,19-docosaheptaenoate	1000336-80-3
Methanesulfonyl chloride	124-63-0	4,4-Dimethyl-3-(3-methylbut-3-enylidene)-2-methylenebicyclo[4.1.0]heptane	79718-83-5
1,2-Ethanediol, 1,2-di-4-pyridinyl-	6950-04-5	Methyl ethyl cyclopentene	19780-56-4
Piconol	586-98-1	.beta.-Longipinene	41432-70-6

Tentative identifications of the most abundant peaks found in heated JUUL or Calm Vape and not found in unheated products.

Table E3: Summary of comparisons for male vs female mice for all parameters measured.

Study Outcomes	Markers	CBD-vape Male vs Female
1. Lung Damage	Total Protein levels in BAL	Equivalent
	FITC-dextran levels in blood	Equivalent
	Albumin levels in BAL	Equivalent
	Neutrophil Elastase levels in BAL	Equivalent
	Neutrophil Elastase levels in lungs	Equivalent
	MPO activity in BAL	Equivalent
	MPO activity in lungs	Equivalent
2. Inflammatory Markers	IL-6	Equivalent
	IL1-alpha	Equivalent
	G-CSF	Equivalent
	IL-5	Equivalent
	KC	Equivalent
	IL-2	Equivalent
	IL-10	Equivalent
3. Immune cells	IFN-g	Equivalent
	Total lung immune infiltrate	Equivalent
	#Neutrophils	Equivalent
	#CD8 ⁺ T cells	Equivalent
	#CD4 ⁺ T cells	Equivalent
	#CD19 ⁺ B Cells	Equivalent
	#CD4 ⁺ IL-17A ⁺ T Cells	Equivalent
	#CD4 ⁺ RORgt ⁺ T Cells	Equivalent
	#CD4 ⁺ Foxp3 ⁺ T Cells	Equivalent
	#CD11c ⁺ Siglec-F ⁺ macrophages	Equivalent
	#CD11c ⁺ CD206 ⁺ interstitial macrophages	Equivalent
	#CD11c ⁺ Arginase-1 ⁺ macrophages	Equivalent
4. Oxidative Stress	Total antioxidant levels in lungs and BAL	Equivalent

Table E4: Detailed list (vendor, marker, fluorophore, and catalogue number) of various fluorochrome-conjugated antibodies used in this study.

Panel of antibodies for lymphoid cells				
No	Vendor	Marker	Fluorophore	Cat no
1	Biogend	CD3	APC-Cy7	100222
2	BD	CD45	BUV395	564279
3	Ebiosciences	CD19	SB 600	63-0193-82
4	Biogend	CD8	PE-Cy7	100722
5	Ebiosciences	CD4	eFluor-450	48-0042-82
6	Invitrogen	IL-17 A	PerCpCy5.5	45-7177-82
7	Ebiosciences	Royt	PE	12-6988-82
8	ThermoFisher/InV	Foxp3	Alexa-488	53-5773-82
9	Biogend	live/dead	Zombie UV	423108
Panel of antibodies for myeloid cells				
No	Ventor	Marker	Fluorophore	Cat no
1	BD	F/480	BV510	BD 743280
2	BD	CD45	BUV395	BD 564279
3	Ebiosciences	CD11b	Ax700	56-0112-82
4	Biogend	CD68/IC	PE	137014
5	ThermoFisher	Siglec-F	SB600	63-1702-82
6	BD	CD11c	APC-Cy7	561241
7	Biogend	CD206	Percp Cy5.5	141716
8	ThermoFisher	Arginase-1/IC	Efluor-450	48-3697-82
9	ThermoFisher	Inos/IC	PE-Cy7	25-5920-82
10	Ebiosciences	Ly6G	FITC	11-5931-85
11	Biogend	live/dead	Zombie UV	423108

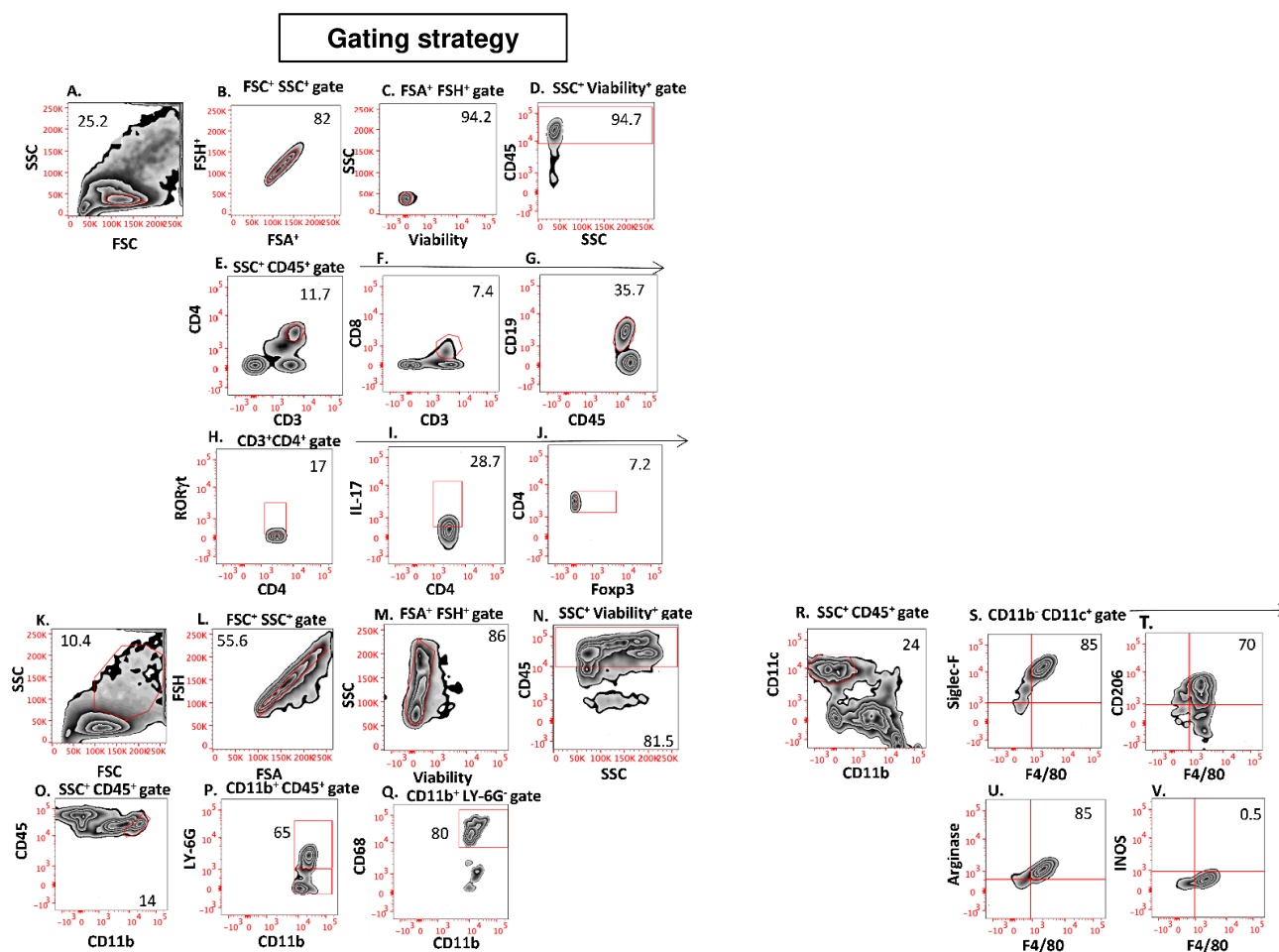


Figure E5. Stepwise gating strategy for the analysis of various cell types based on fluorophore markers used in flow cytometry.

Representative plots showing the gating strategy adopted for the step-by-step analysis of different immune cell subsets from lung tissue. Lung cells were gated based on (A) FSC-SSC (lymphoid) and subsequently by FSA-FSH gate (singlets) (B), SSC⁺-Viability⁺ gate (C), SSC⁺CD45⁺gate (D). SSC⁺CD45⁺ population were further gated for CD3⁺CD4⁺ T cells (E), CD3⁺CD8⁺ T cells (F), CD45⁺CD19⁺ B cells (G). CD3⁺CD4⁺ T cells are further gated for RORγt⁺ (H), IL-17⁺ (I), and Foxp3⁺CD4⁺ T cells (J). Myeloid cells were gated based on (K) FSC-SSC and subsequently by FSA-FSH gate (singlets) (L), SSC-Viability⁺ gate (M), SSC⁺CD45⁺gate (N), CD11b⁺CD45⁺ (O), CD11b⁺CD45⁺ population were further gated for CD11b⁺LY-6G⁺ neutrophils and LY-6G⁻ cells (P). Ly-

6G⁻ population were gated for CD11b⁺CD68⁺ macrophages (**Q**). SSC⁺CD45⁺ cells were again gated for CD11b⁻CD11c⁺ (**R**). CD11b⁻CD11c⁺ cells are gated for F4/80⁺ Siglec-F⁺ (**S**), F4/80⁺ CD206⁺ (**T**), F4/80⁺ Arginase-1⁺ (**U**), and F4/80⁺ INOS⁺ (**V**). Numbers indicate the frequencies of respective immune cell subsets gated.

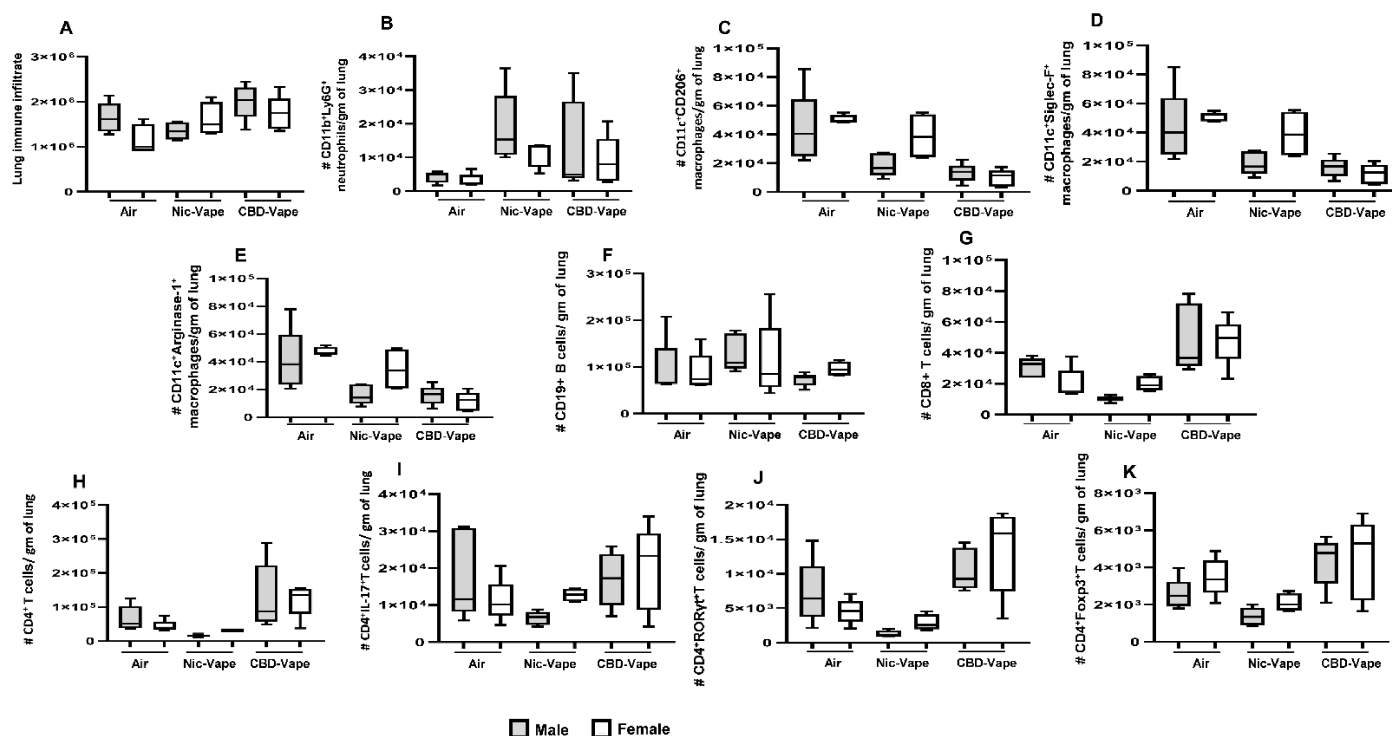


Figure E6. Differential influence of sex on lung infiltration of selective immune cell subsets following inhalation exposure to nicotine or CBD aerosols.

Lung immune infiltrate (A), CD11b⁺Ly6G⁺ neutrophils (B), CD11b⁻CD11c⁺CD206⁺ macrophages (C), CD11b⁻CD11c⁺Siglec-F⁺ macrophages (D), CD11b⁻CD11c⁺arginase⁺ macrophages (E), CD19⁺ B cells (F), CD8⁺ T cells (G), CD4⁺ T cells (H), CD4⁺IL17A⁺ T cells (I), CD4⁺RORγt⁺ T cells (J) and CD4⁺FOXP3⁺ T cells (K). Data are shown as box plots with whiskers at min and max. Difference between two groups was considered significant at P value <0.05 after performing Kruskal-Wallis non-parametric test with FDR correction for multiple comparisons by GraphPad Prism 9 software (GraphPad; La Jolla, CA). In each experiment $n=10$ (5 males + 5 females) (for nicotine $n=9$ (5 males + 4 females)) mice per group.

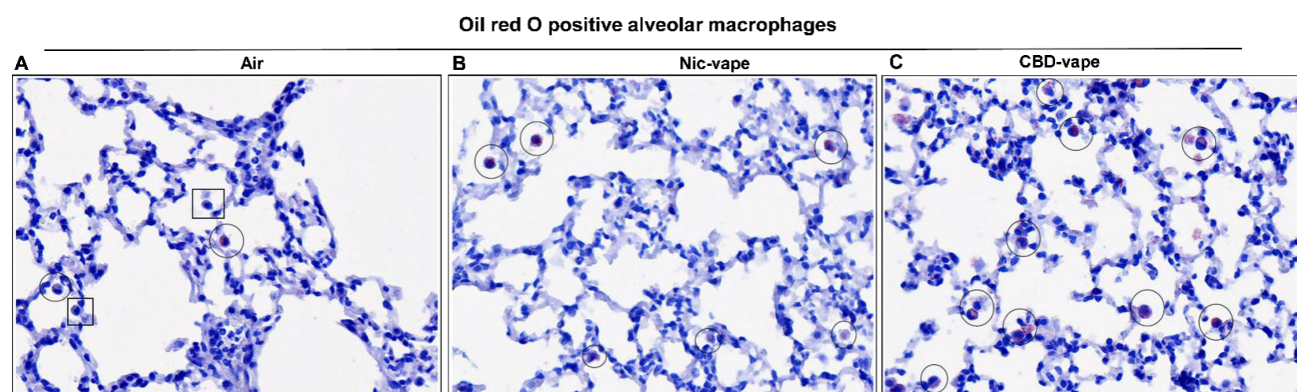


Figure E7. Induction of rare lipid-containing intra-alveolar macrophages following inhalation exposure to CBD and nicotine aerosols.

(A) Air: A single lipid containing macrophage is found in two non-adjacent alveoli (circles) in control lungs. Non-lipid containing alveolar macrophages are also present (box). Oil red O, 40x magnification.

(B) Nicotine-containing vaping product (Nic-vape) and (C) CBD-containing vaping products (CBD-vape): One or more lipid containing macrophages are found in multiple, often adjacent alveoli (circles). Oil red O, 40x magnification.

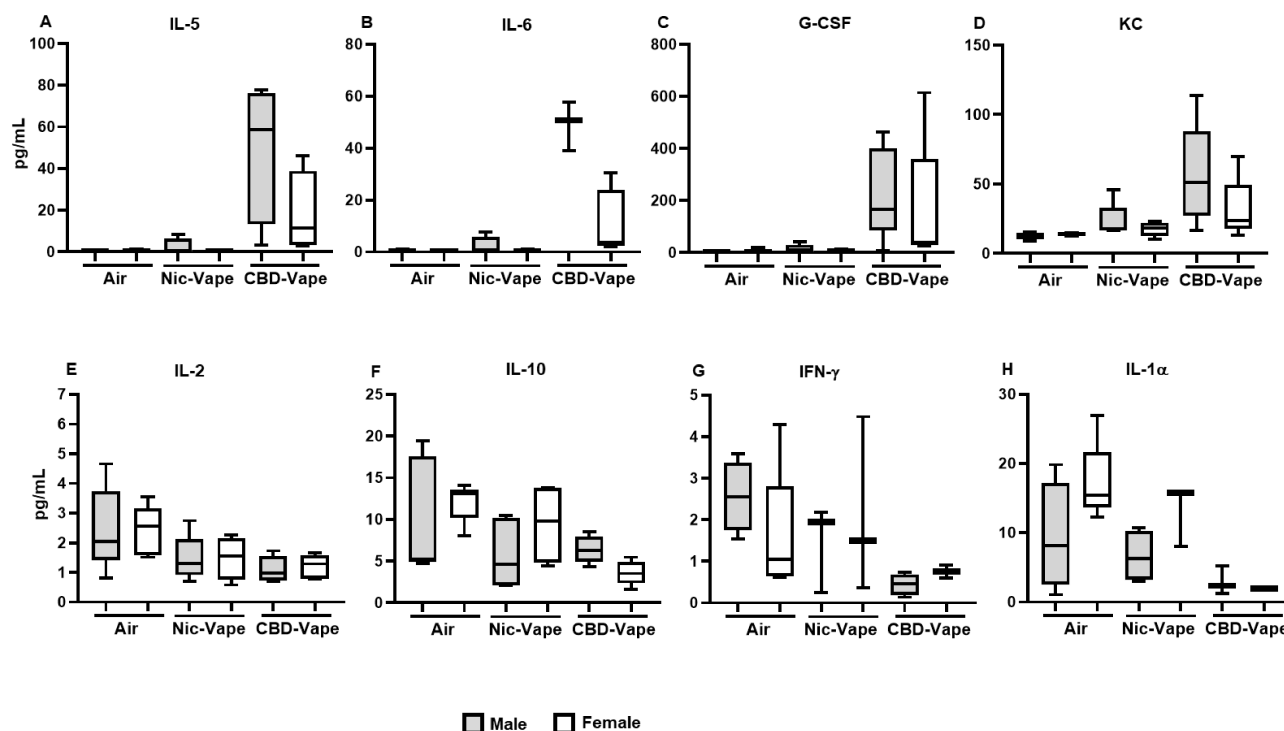


Figure E8. Levels of inflammatory cytokines/chemokines in the BAL fluid of male vs female mice following inhalation of CBD and nicotine aerosols.

Levels of inflammatory cytokines and chemokines in the BAL (**A-H**) of mice after 2 wks of exposure to air, Nic-Vape or CBD-Vape aerosols were quantified using MILLIPLEX MAP Kit as described in materials and methods. Data are shown as box plots with whiskers at min and max. One-way ANOVA with Tukey's post-test comparison was performed by GraphPad Prism 9 software (GraphPad; La Jolla, CA) and the difference between two groups is considered significant at P value <0.05 calculated after performing non-parametric Kruskal-Wallis test with FDR correction for multiple comparisons by employing GraphPad Prism 9 software (GraphPad; La Jolla, CA). In each experiment $n=10$ (5 males + 5 females) (for nicotine $n=9$ (5 males + 4 females)) mice per group.

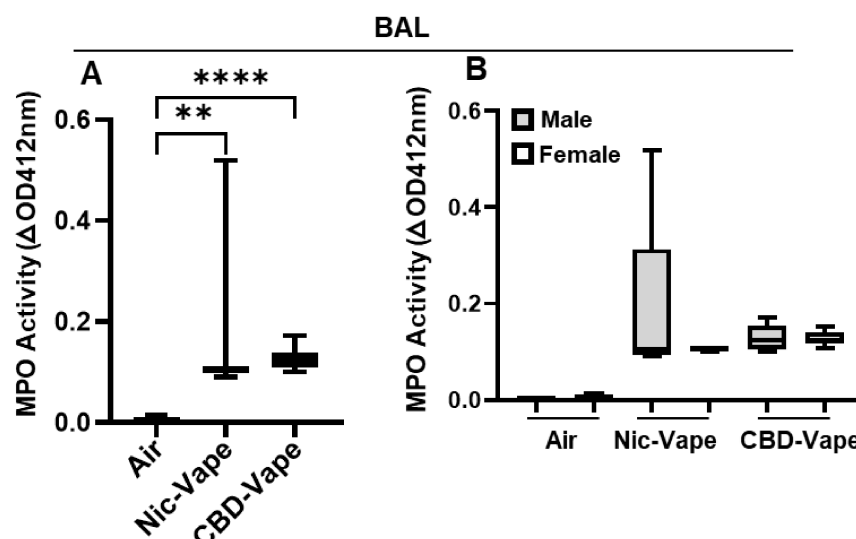


Figure E9. Myeloperoxidase (MPO) activity in the BAL following inhalation exposure to CBD and nicotine aerosols.

After acute exposures to CBD or nicotine aerosols ended, mice were euthanized, and the BAL fluid was harvested. (A-B) MPO activity in the BAL samples of nicotine or CBD aerosol-exposed animals was measured using MPO assay kit from Abcam (Cat# ab105136) as described in detail in the supplemental methods section. Data are shown as box plots with whiskers at min and max.

Difference between two groups was considered significant at P value <0.05 , statistical significance of the difference between two groups is indicated with symbols $**P<0.01$; $****P<0.0001$ after performing non-parametric Kruskal-Wallis test with FDR correction for multiple comparisons used to see if statistically significant differences exist between the two groups using GraphPad Prism 9 software (GraphPad; La Jolla, CA). In each experiment $n=10$ (5 males + 5 females) (for nicotine $n=9$ (5 males + 4 females)) mice per group.

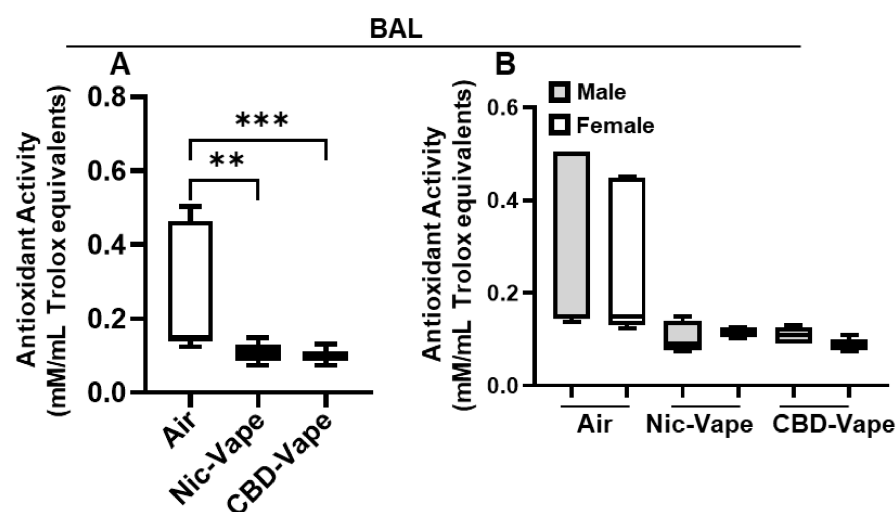


Figure E10. Changes in antioxidant potential in the BAL following inhalation exposure to CBD and nicotine aerosols.

At the end of the acute exposures, mice were euthanized, and the BAL was harvested. (**A-B**) Total antioxidant levels in the BAL were quantified using antioxidant assay kit from Cayman Chemical (Cat# 709001). Details of the assay are described in the supplemental material section. Data are shown as box plots with whiskers at min and max. Difference between two groups of mice was considered significant at P value ≤ 0.05 , statistical significance of the difference between two groups is indicated with symbols $**P < 0.01$; $***P < 0.001$ after performing non-parametric Kruskal-Wallis test with FDR correction for multiple comparisons by GraphPad Prism 9 software (GraphPad; La Jolla, CA). In each experiment $n=10$ (5 males + 5 females) (for nicotine $n=9$ (5 males + 4 females)) mice per group.

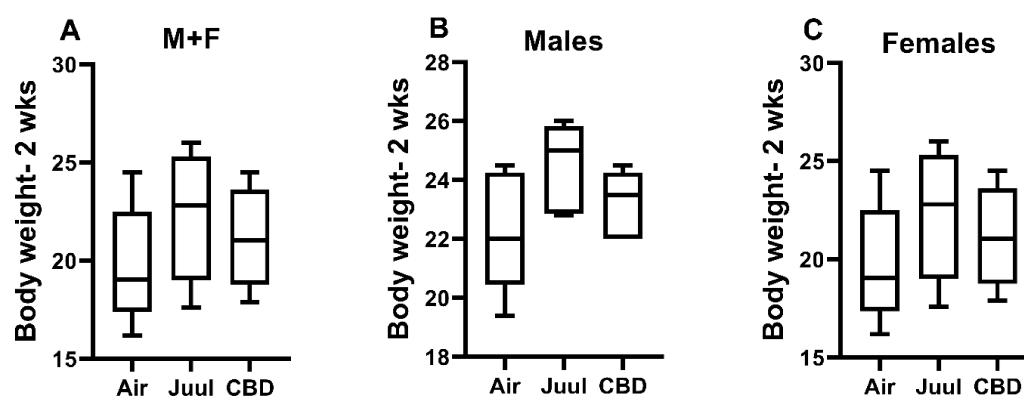


Figure E11. Animal body weights after 2-week inhalatory exposure to CBD and nicotine aerosols.

At the end of exposures, mice were euthanized, and animal weights measured. (**A-C**) Total body weights (in grams) of mice in each group. Data are shown as box plots with whiskers at min and max. Difference between two groups of mice was considered significant at P value <0.05 , statistical significance of the difference between two groups was calculated by performing non-parametric Kruskal-Wallis test with FDR correction for multiple comparisons by GraphPad Prism 9 software (GraphPad; La Jolla, CA). In each experiment $n=10$ (5 males + 5 females) (for nicotine $n=9$ (5 males + 4 females)) mice per group.

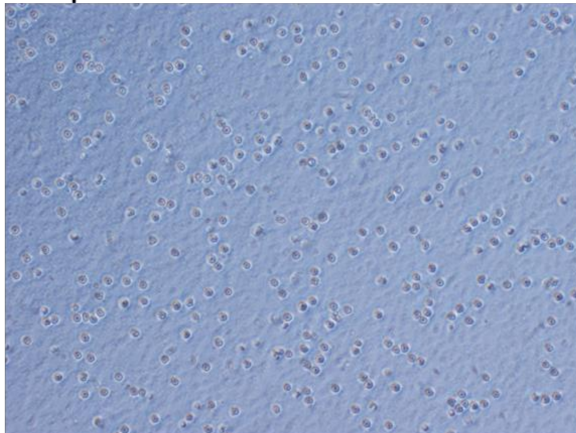
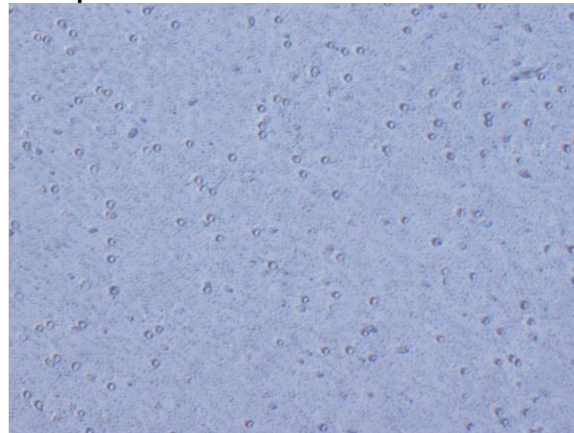
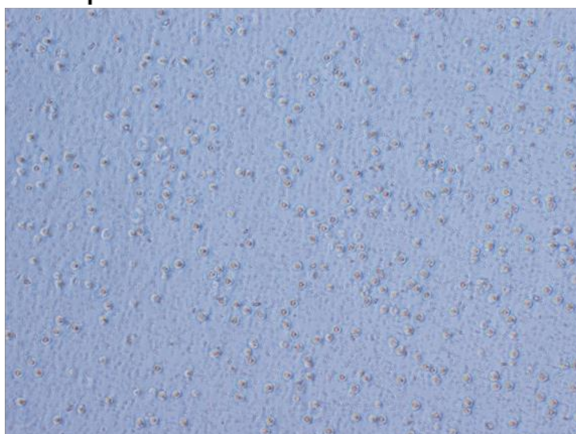
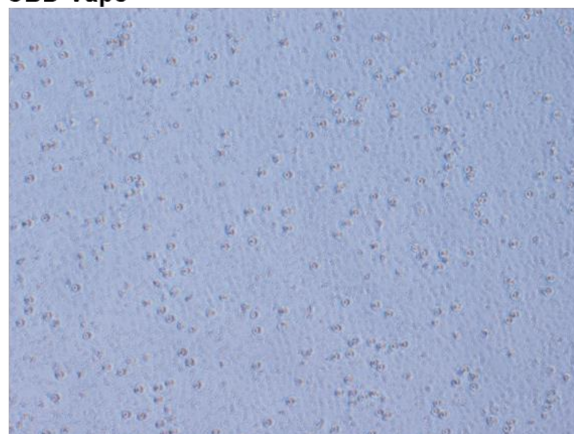
Unexposed**Air-exposed****Nic-Vape****CBD-Vape**

Figure E12. Human neutrophils purified from whole blood were seeded at 0.8 million cells/culture insert in a 6-well plate format and immediately exposed to 110 puffs of Air, nicotine (50 mg/mL nicotine) or CBD (50 mg/mL)-containing aerosols at the air-liquid interface in a 55 mL puff volume as described in methods. At the end of the exposures, cells were removed from the ALI chamber and recovered in complete growth media for 24 hours. Cells were then pictured at 200x in a phase-contrast microscope (Olympus IX73) before harvesting them for various assays.